Recent Research and Developments Related to Near-Equiatomic Titanium-Platinum Alloys for High-Temperature Applications

Effect of partial substitution of titanium and platinum in $Ti_{50}Pt_{50}$ on strength and shape memory properties above 800°C

By Abdul Wadood* and Yoko Yamabe-Mitarai

High Temperature Materials Unit, National Institute for Materials Science (NIMS) 1-2-1 Sengen, Tsukuba, Ibaraki 305-0047, Japan

*Email: wadood.abdul@nims.go.jp; wadood91@gmail.com

Titanium-platinum ($Ti_{50}Pt_{50}$) (all compositions in at%) alloy exhibits thermoelastic martensitic phase transformation above 1000°C and has potential for high-temperature shape memory material applications. However, as has been previously reported, $Ti_{50}Pt_{50}$ alloy exhibited a negligible recovery ratio (0–11%) and low strength in martensite and especially in the austenite phase due to low critical stress for slip deformation. In order to improve the high-temperature strength and shape memory properties, the effects of partial substitution of Ti with other Group 4 elements such as zirconium and hafnium and the effect of partial substitution of Pt with other platinum group metals (pgms) such as iridium and ruthenium on the high-temperature mechanical and shape memory properties of $Ti_{50}Pt_{50}$ alloy were recently investigated. This paper reviews the transformation temperatures and high-temperature mechanical and shape memory properties of recently developed Ti site substituted $(Ti,Zr)_{50}Pt_{50}$, $(Ti,Hf)_{50}Pt_{50}$ and Pt site substituted $Ti_{50}(Pt,Ru)_{50}$ and $Ti_{50}(Pt,Ir)_{50}$ alloys for high-temperature (~800°C–1100°C) material applications.

1. Introduction

Equiatomic nickel-titanium (NiTi), also known as nitinol, is one of the best-known shape memory alloys. However, nitinol is limited to biomedical and room temperature engineering applications (1) and cannot be used at high temperature (for example, above 100°C) due to its low transformation temperature (2–4). Recently, partial substitution of Ni with Pt and Pd in NiTi was found to be effective for increasing the transformation temperature and it was reported that recently developed NiTi-Pd (5) and NiTi-Pt (6) have potential for high-temperature

shape memory material applications (4). $Ti_{50}Pd_{50}$ and $Ti_{50}Pt_{50}$ exhibit a thermoelastic orthorhombic (B19) martensitic phase transformation from the austenite (B2) phase. Austenite finish (A_f) (1085ºC) and martensite finish (M_f) (1020ºC) temperatures of $Ti_{50}Pt_{50}$ were found to be ~500ºC higher than those of $Ti_{50}Pd_{50}$ whose A_f was 550ºC and M_f was 480ºC (7). Thus, $Ti_{50}Pt_{50}$ can be used for much higher temperature (for example, above 1000ºC) shape memory material applications than $Ti_{50}Pd_{50}$, which can be used for 400ºC–600ºC applications (5). $(Ti,Zr)_{50}Pd_{50}$ (8) has a M_f of 445ºC, lower than that of $Ti_{50}Pd_{50}$ (5, 7), showing that Zr acts as a B2 phase stabiliser in $Ti_{50}Pd_{50}$. Transformation temperatures of $Ti_{50}Pd_{50}$ (7), $Ti_{50}Au_{50}$ (9, 10), $Ti_{50}Pt_{50}$ (7) and $Ti_{50}Ni_{50}$ (3) are given in **Table I**. As shown in **Table I**, $Ti_{50}Pt_{50}$ (7) alloy has the highest transformation temperature among the four alloys. Only $Ta_{50}Ru_{50}$ and $Nb_{50}Ru_{50}$ (11, 12) have high transformation temperatures similar to $Ti_{50}Pt_{50}$ alloy (4, 7). $Ta_{50}Ru_{50}$ and $Nb_{50}Ru_{50}$ exhibit two-stage transformation from B2 to tetragonal β' phase, and then from β' to monoclinic β'' phase at low temperature (12), whereas $Ti_{50}Pt_{50}$ (7) exhibits one-stage transformation from B2 phase to thermoelastic orthorhombic (B19) martensitic phase (7).

Biggs *et al*. found diffusionless twin oriented martensitic transformation at about 1000ºC in $Ti_{50}Pt_{50}$ alloy. Broad laths with well-developed midribs were observed close to the equiatomic composition (13). They also showed that the B2 (austenite) to B19 (martensite) phase field ranges from 46 at% to 54 at% Pt (14). Ti_4Pt_3 phase, which had not been reported before, was shown to be 30%–45% Pt in the revised phase diagram for TiPt and the phase boundary for TiPt agreed well with the literature (15). The site preference behaviour of solute addition to TiPd and TiPt on the basis of theoretical calculations of

energy gap was provided by Bozzolo *et al*. (16). The phase stability of TiPt at equiatomic composition was investigated theoretically using the heat of formation, elastic properties, electronic structure (density of states) and phonon dispersion curves of B2, B19 and B19' structures (17). The partial isothermal section of the Al-Ti-Pt phase diagram at 1100ºC was studied in the compositional region below 50 at% Pt (18).

Due to the high transformation temperature of the $Ti_{50}Pt_{50}$ alloy (4, 7, 14), the room temperature to high-temperature (for example, 50ºC below M_f and 50ºC above A_f) mechanical properties and shape memory properties of Ti site substituted and Pt site substituted $Ti_{50}Pt_{50}$ alloy were investigated. This article discusses and compares recently reported results from the present group related to the phase transformation temperatures, mechanical and shape memory properties of $Ti_{50}Pt_{50}$, Ti site substituted $(Ti,Zr)_{50}Pt_{50}$, $(Ti,Hf)_{50}Pt_{50}$ and Pt site substituted $Ti_{50}(Pt,Ir)_{50}$ and $Ti_{50}(Pt,Ru)_{50}$ alloys.

2. Experimental Procedures

Alloys were created by arc melting, homogenised at 1250ºC for 3 h, and then quenched with ice water. The phase transformation temperatures were investigated using differential thermal analysis (DTA) between 600ºC to 1100ºC at a heating and cooling rate of 10ºC min⁻¹ using a Shimadzu DTA-50 device. X-ray diffraction analysis was conducted at room temperature (~25ºC) to high temperature from 20º–90º in 2θ using a Rigaku TTR-III X-ray diffractometer with CuKα radiation. For microstructural observation, sputter etching (dry etching) was carried out using a glow discharge optical emission spectrometer (GD-OES) and argon-nitrogen gas mixture. For shape memory effect measurements, rectangular samples of 2.5 mm × 2.5 mm × 5 mm were compressed to apply 5% strain at a temperature of

Table I

Transformation Temperatures of $Ti_{50}Au_{50}$ (9), $Ti_{50}Pd_{50}$ (7), $Ti_{50}Pt_{50}$ (7) and $Ti_{50}Ni_{50}$ (3) Alloys

Alloy	M_s, ºC	M_f,ºC	A_s, ºC	A_f, ºC	A_f–M_f, ºC
$Ti_{50}Au_{50}$ (9)	597	586	615	624	38
$Ti_{50}Pd_{50}$ (7)	510	480	520	550	70
$Ti_{50}Pt_{50}$ (7)	1070	1020	1040	1085	65
$Ti_{50}Ni_{50}$ (3)	−19	−33	−4	7	40

50ºC below M_f using a Shimadzu AG-X compression test system. Samples were then heated to 1250ºC and held for 1 h under vacuum for shape recovery. The shape memory effect was measured by comparing the sample's length before deformation, after applying 5% strain and after heat treatment. For mechanical testing, cyclic loading–unloading compression tests were conducted for 20% applied strain at test temperatures of 50ºC below M_f and 50ºC above A_f with an initial strain rate of 3×10^{-4} s^{-1}.

3. Results and Discussion

3.1 Ti$_{50}$Pt$_{50}$ Alloys

The transformation temperatures of Ti$_{50}$Pt$_{50}$ alloy reported by the present research group (19) were found to be ~50ºC less than those reported elsewhere (7). A 50ºC difference in transformation temperatures is expected to be due to small composition variations, accuracy or the type and distance of the thermocouple from the specimen and experimental method used. The B2 phase structure was identified for Ti$_{50}$Pt$_{50}$ alloy above A_f and B19 martensitic phase was identified below M_f and the lattice parameters of B19 and B2 increased with increasing temperature (20). The lattice parameters of B19 and B2 reported by the present research group (20) were found to be close to those reported by H. C. Donkersloot and J. H. N. Van Vucht (7), as shown in **Table II**. The stress for reorientation of martensite at room temperature was found to be 200 MPa, decreasing to 50 MPa when tested at 50ºC below M_f of Ti$_{50}$Pt$_{50}$ alloy (20). The small non-linear strain recovery upon unloading of mechanically loaded Ti$_{50}$Pt$_{50}$ alloy samples below M_f was related to pseudoelasticity caused by the reversion of a small fraction of detwinned martensite to twinned martensite upon unloading (20). In the case of superelasticity, there is reverse transformation of deformation-induced martensite to the parent austenite phase upon unloading.

It was also found (19) that Ti$_{50}$Pt$_{50}$ alloy exhibited negligible shape memory effect (~11%), due to the low critical stress for slip deformation compared to the stress required for martensite reorientation. The Ti$_{50}$Pt$_{50}$ alloy exhibited the single yielding phenomenon and very low strength (20 MPa) in the B2 phase region (19). Thus, Ti$_{50}$Pt$_{50}$ alloy is very soft in the B2 phase region. The single yielding phenomenon showed that slip is the dominant deformation mechanism. The drastic decrease in strength during phase transformation from B19 to B2 and negligible shape memory effect demonstrate that Ti$_{50}$Pt$_{50}$ cannot be used for high-temperature shape memory material applications. The effect of partial substitution of Ti with the Group 4 metals Zr and Hf and of Pt with Ir and Ru to improve the high-temperature strength and shape memory properties are reviewed here.

3.2 Ti$_{50}$(Pt,Ir)$_{50}$ Intermetallic Alloys

Ir has a high melting point (2447ºC) compared to Pt (1769ºC) (21). Both Pt and Ir have the face-centred cubic (fcc) crystal structure (22). The solubility of Ir in TiPt is expected to be high as Ir is a pgm. Ir was therefore selected to improve the high-temperature strength and shape memory properties of Ti$_{50}$Pt$_{50}$ alloy. The nominal compositions of developed alloys were: Ti$_{50}$(Pt$_{37.5}$Ir$_{12.5}$), Ti$_{50}$(Pt$_{25}$Ir$_{25}$) and Ti$_{50}$(Pt$_{12.5}$Ir$_{37.5}$) (19, 23–25). It was found that the intensity of DTA peaks became weaker and the peak width became wider with increasing Ir content (23). As shown in **Figure 1**, the phase transformation temperatures were also increased by partial substitution of Pt with Ir and A_f, which was 1057ºC for Ti$_{50}$Pt$_{50}$ alloy, was

Table II

Lattice Parameters B19 and B2 of Ti$_{50}$Pt$_{50}$ at Different Temperatures

Alloy	Temperature	Phase	a, Å	b, Å	c, Å
Ti$_{50}$Pt$_{50}$ (20)	RT	B19	4.586	2.761	4.829
	1200°C	B2	3.191	–	–
	1300°C		3.196	–	–
Ti$_{50}$Pt$_{50}$ (7)	RT	B19	4.55	2.73	4.79
	1100°C	B2	3.192	–	–
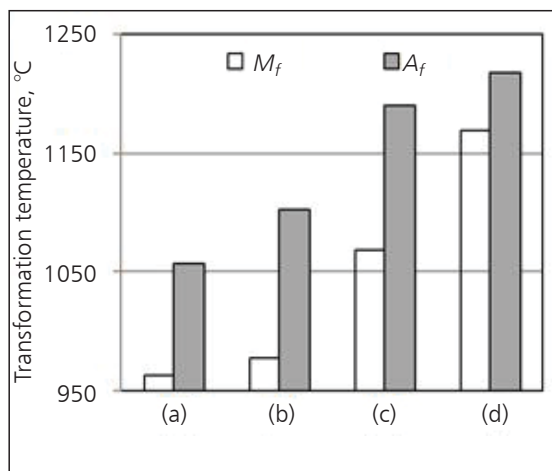
Fig. 1. Transformation temperatures (19) of: (a) $Ti_{50}Pt_{50}$; (b) $Ti_{50}(Pt_{37.5}Ir_{12.5})$; (c) $Ti_{50}(Pt_{25}Ir_{25})$; (d) $Ti_{50}(Pt_{12.5}Ir_{37.5})$

increased to 1218ºC for $Ti_{50}(Pt_{12.5}Ir_{37.5})$ alloy (19). The transformation temperatures were increased by approximately 4ºC for 1 at% partial substitution of Pt with Ir (19, 25). The lattice parameter of B2 phase in $Ti_{50}Pt_{50}$ was decreased with increasing Ir content up to $Ti_{50}(Pt_{25}Ir_{25})$. However, as the Ir content was increased further, the lattice parameter of B2 phase increased (25). Because the B19 phase is an orthorhombic structure, the lattice parameter ratios a/b, c/b and c/a were found to be larger than 1.0 and the largest values of a/b, c/b and c/a appeared in $Ti_{50}Pt_{50}$ and decreased with increasing Ir content. When the crystal structure is tetragonal, according to the adopted formula $a = c \neq b$ lattice parameters a and c will have the same value, whereas b will have different values and c/a should be 1.0 (25). It was shown that the value of c/a approached 1 for $Ti_{50}(Pt_{20}Ir_{30})$ alloy, indicating that the orthorhombic martensitic structure of $Ti_{50}Pt_{50}$ changed to a tetragonal phase with increasing Ir content to ~30 at% Ir in $Ti_{50}(Pt,Ir)_{50}$ alloys (25). Based on these results, the $Ti_{50}(Pt,Ir)_{50}$ alloys were divided into three groups. The first group for the alloys with Ir of up to approximately 10% was considered to be the $Ti_{50}Pt_{50}$ type orthorhombic structure because the lattice parameters and the lattice parameter ratios were close to those of $Ti_{50}Pt_{50}$. In the second group with Ir content of 10 at% to 30 at%, the orthorhombic structure changed to nearly tetragonal with increasing Ir content. In the third group, the Ir content of alloys was above 30 at% Ir, where the lattice parameter ratio c/a once again increased with increasing Ir content (25).

Microstructural analysis was used to observe the surface relief around the phase transformation temperature for $Ti_{50}Pt_{50}$ as well as $Ti_{50}(Pt,Ir)_{50}$ alloys. However, the surface relief, which was very clear in $Ti_{50}Pt_{50}$, became less clear in $Ti_{50}(Pt,Ir)_{50}$ alloys (24). The compressive strength at 1000ºC test temperature of $Ti_{50}Pt_{50}$ (300 MPa) increased to ~1000 MPa for $Ti_{50}(Pt_{12.5}Ir_{37.5})$ alloy as shown in **Figure 2** (24). Another study indicates that $Ti_{50}Pt_{50}$ exhibits the single yielding phenomenon (19). However, shape memory alloys exhibit double yielding, where the first yielding is related to deformation-induced martensitic transformation and the second yielding is related to permanent deformation due to slip (26). The single yielding phenomenon for $Ti_{50}Pt_{50}$ showed that slip is the dominant deformation mechanism (19).

The double yielding phenomenon, which is a characteristic of shape memory alloys (26), was analysed for $Ti_{50}(Pt,Ir)_{50}$ alloys (19, 24). A maximum recovery ratio of 57% due to the shape memory effect was observed for $Ti_{50}(Pt_{25}Ir_{25})$ alloy after deformation at 850ºC and then heating above A_f (24, 25) as shown in **Figure 2**. However, the recovery ratio due to the shape memory effect decreased with further increase in Ir content (24, 25). $Ti_{50}Pt_{50}$ in the austenitic phase region exhibited very low strength (~20 MPa) when compression tested at 50ºC above A_f (19). It was also shown that the strength of $Ti_{50}Pt_{50}$ alloy in the austenitic phase region was increased from 20 MPa to 240 MPa by partial substitution of Pt with Ir in $Ti_{50}(Pt_{12.5}Ir_{37.5})$
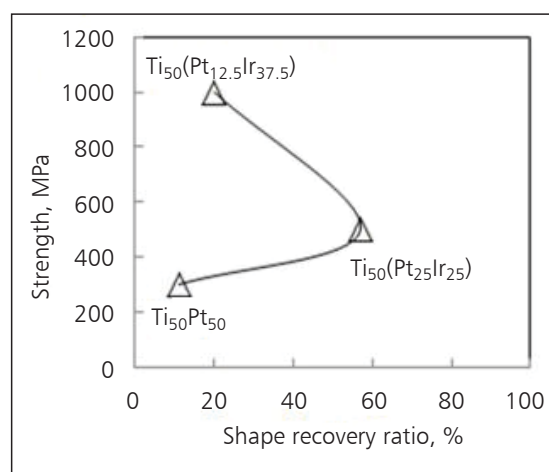

Fig. 2. Strength of martensite at 1000ºC shape recovery ratio of TiPt and TiPt-Ir alloys (24)

alloys (19). However, the strength of $Ti_{50}(Pt,Ir)_{50}$ alloy in the B2 phase region was still much lower than that in the martensite phase region (~1000 MPa) (24); further research is required to improve the strength of $Ti_{50}Pt_{50}$ shape memory alloys.

3.3 TiPt-Zr, TiPt-Hf and TiPt-Ru Intermetallic Alloys

The transformation temperatures, high-temperature mechanical and shape memory properties of Ti site substituted $(Ti_{45}Zr_5)Pt_{50}$ (27, 28), $(Ti_{45}Hf_5)Pt_{50}$ (29) and Pt site substituted $Ti_{50}(Pt_{45}Ru_5)$ (27) shape memory alloys have recently been reported. Similar to Ti, Zr and Hf also belong to Group 4 of the periodic table, so Zr and Hf have the same number of valence electrons (i.e. four) as Ti. The group number, melting point, density and atomic radius of Ti, Zr, Hf, Ru and Ni are listed in **Table III**. As shown, the atomic radii of Zr and Hf are larger than that of Ti (30), so partial substitution of Ti with Zr and/or Hf is expected to improve the high-temperature strength and shape memory properties of $(Ti_{45}Zr_5)Pt_{50}$ and $(Ti_{45}Hf_5)Pt_{50}$ alloys due to the solid solution strengthening effect. Similar to Pt, Ru is also a pgm, its atomic radius is smaller than that of Pt (30). The density of Ru is also lower than that of Pt. The melting points of Hf and Zr are higher than that of Ti and the melting point of Ru is higher than that of Pt (**Table III**). Therefore, partial substitution of Ti with Zr and/or Hf in $(Ti_{45}Zr_5)Pt_{50}$ and $(Ti_{45}Hf_5)Pt_{50}$ alloys, as well as partial substitution of Pt with Ru in $Ti_{50}(Pt_{45}Ru_5)$ alloys is expected to increase the melting temperature

of $Ti_{50}Pt_{50}$ alloys. The densities of Zr and Hf are higher than that of Ti, so partial substitution of Ti with Zr and/or Hf will increase the density of $Ti_{50}Pt_{50}$ alloy. However, the effect will be small for partial substitution of Ti with Zr compared to partial substitution of Ti with Hf due to the small density difference between Ti and Zr compared to that between Ti and Hf. Since Ru is less dense than Pt, partial substitution of Pt with Ru will decrease the density of $Ti_{50}Pt_{50}$ alloy. It was reported (27–29) that partial substitution of Ti with Zr and Hf, as well as partial substitution of Pt with Ru in $Ti_{50}Pt_{50}$ alloy, effectively improved the strength in the martensitic phase as well as in the austenitic (B2) phase region when tested at 50ºC below M_f and 50ºC above A_f. The strength at 50ºC below M_f and 50ºC above A_f of $Ti_{50}Pt_{50}$ (19), $(Ti_{45}Zr_5)Pt_{50}$ (27, 28), $(Ti_{45}Hf_5)Pt_{50}$ (28, 29) and $Ti_{50}(Pt_{45}Ru_5)$ (27) alloys is given in **Figure 3**. Partial substitution of Ti with Zr in $Ti_{50}Pt_{50}$ was found to be more effective in improving the strength and shape memory properties (27, 28) than partial substitution of Ti with Hf (28, 29) and partial substitution of Pt with Ru (27). As revealed by the energy dispersive spectroscopy (EDS) composition analysis of matrix and precipitates (27), partial substitution of Ti with Zr in $(Ti_{45}Zr_5)Pt_{50}$ results in precipitation of $(Ti,Zr)Pt_3$. Such precipitates were not found for $(Ti_{45}Hf_5)Pt_{50}$ (28, 29) and $Ti_{50}(Pt_{45}Ru_5)$ (27) alloys, so the higher strength and shape memory properties for $(Ti_{45}Zr_5)Pt_{50}$ were due to the combined effects of solid solution strengthening and $(Ti,Zr)Pt_3$

Table III

Physical Properties of Ti, Zr, Hf, Pt, Ru and Ni Metals

Metal	Group number	Atomic radius, nm (30)	Melting point[a], °C	Density at room temperature, g cm^{-3}
Ti	4	0.140	1670	4.5
Zr	4	0.155	1855	6.5
Hf	4	0.155	2231	13.2
Pt	10	0.135	1769	21.3
Ru	8	0.130	2334	12.4
Ni	10	0.135	1453	8.91

[a] *Melting points are given from ASM Alloy Phase Diagram Database*^{TM}
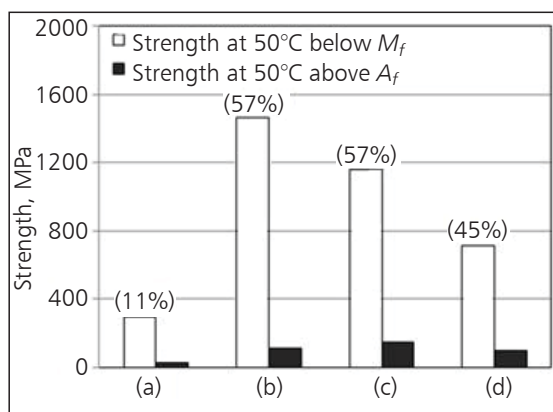
Fig. 3. Strength at 50°C below M_f and 50°C above A_f of: (a) $Ti_{50}Pt_{50}$ (19); (b) $(Ti_{45}Zr_5)Pt_{50}$ (27, 28); (c) $(Ti_{45}Hf_5)Pt_{50}$ (28, 29); and (d) $Ti_{50}(Pt_{45}Ru_5)$ (27) alloys. Shape recovery ratios are given in parentheses

precipitation resulting in an effective increase in critical stress for slip deformation. It was also reported that the transformation temperatures were decreased by partial substitution of Ti with Zr in $(Ti_{45}Zr_5)Pt_{50}$ (27, 28) and by partial substitution of Ti with Hf in $(Ti_{45}Hf_5)Pt_{50}$ (28, 29) alloys, as well as by partial substitution of Pt with Ru in $Ti_{50}(Pt_{45}Ru_5)$ (27) alloys. This showed that Zr, Hf and Ru act as B2 phase stabilisers in $Ti_{50}Pt_{50}$ intermetallic alloys.

4. Conclusions

The potential of equiatomic $Ti_{50}Pt_{50}$ as a high-temperature shape memory alloy was reviewed. Recent efforts to improve the high-temperature mechanical and shape memory properties of $Ti_{50}Pt_{50}$ alloy were also discussed. Partial substitution of Ti with other Group 4 elements such as Zr and Hf, as well as partial substitution of Pt with other pgms such as Ir and Ru, was found to be effective for improving the high-temperature mechanical and shape memory properties of $Ti_{50}Pt_{50}$ alloy. The higher strength and shape memory properties for $(Ti_{45}Zr_5)Pt_{50}$ were related to the combined effects of solid solution strengthening and $(Ti,Zr)Pt_3$ precipitation. It was also reported that the crystal structure of orthorhombic martensite (B19) changed to tetragonal structure with increasing Ir content in $Ti_{50}(Pt,Ir)_{50}$ alloys. 100% shape memory effect has still not been achieved and the strength of the developed TiPt-*X* alloys in the B2 phase is still much lower than that in the martensite phase.

Work is ongoing to solve these challenges in order to use near-equiatomic TiPt based shape memory alloys for high-temperature (>800ºC) applications.

References

1 E. Henderson, D. H. Nash and W. M. Dempster, *J. Mech. Behav. Biomed. Mater.,* 2011, **4**, (3), 261

2 H. Hosoda, S. Hanada, K. Inoue, T. Fukui, Y. Mishima and T. Suzuki, *Intermetallics*, 1998, **6**, (4), 291

3 K. W. K. Yeung, K. M. C. Cheung, W. W. Lu and C. Y. Chung, *Mater. Sci. Eng.: A*, 2004, **383**, (2), 213

4 Y. Xu, S. Shimizu, Y. Suzuki, K. Otsuka, T. Ueki and K. Mitose, *Acta Mater.*, 1997, **45**, (4), 1503

5 O. Rios, R. Noebe, T. Biles, A. Garg, A. Palczer, D. Scheiman, H. J. Seifert and M. Kaufman, *Proc. SPIE*, 2005, **5761**, 376

6 J. Ma, I. Karaman and R. D. Noebe, *Int. Mater. Rev.*, 2010, **55**, (5), 257

7 H. C. Donkersloot and J. H. N. Van Vucht, *J. Less-Common Met.*, 1970, **20**, (2), 83

8 M. Kawakita, M. Takahashi, S. Takahashi and Y. Yamabe-Mitarai, *Mater. Lett.*, 2012, **89**, 336

9 C. Declairieux, A. Denquin, P. Ochin, R. Portier and P. Vermaut, *Intermetallics*, 2011, **19**, (10), 1461

10 T. Kawamura, R. Tachi, T. Inamura, H. Hosoda, K. Wakashima, K. Hamada and S. Miyazaki, *Mater. Sci. Eng.: A*, 2006, **438–440**, 383

11 B. H. Chen and H. F. Franzen, *J. Less-Common Met.*, 1990, **157**, (1), 37

12 R. W. Fonda, H. N. Jones and R. A. Vandermeer, *Scr. Mater.*, 1998, **39**, (8), 1031

13 T. Biggs, M. B. Cortie, M. J. Witcomb and L. A. Cornish, *Metall. Mater. Trans. A*, 2001, **32**, (8), 1881

14 T. Biggs, M. J. Witcomb and L. A. Cornish, *Mater. Sci. Eng.: A*, 1999, **273–275**, 204

15 T. Biggs, L. A. Cornish, M. J. Witcomb and M. B. Cortie, *J. Alloys Compd.*, 2004, **375**, (1–2), 120

16 G. Bozzolo, H. O. Mosca and R. D. Noebe, *Intermetallics*, 2007, **15**, (7), 901

17 R. Mahlangu, M. J. Phasha, H. R. Chauke and P. E. Ngoepe, *Intermetallics*, 2013, **33**, 27

18 O. V. Zaikina, V. G. Khorujaya, D. Pavlyuchkov, B. Grushko and T. Ya. Velikanova, *J. Alloys Compd.*, 2011, **509**, (28), 7565

19 Y. Yamabe-Mitarai, T. Hara, S. Miura and H. Hosoda,

Mater. Trans., 2006, **47**, (3), 650

20 Y. Yamabe-Mitarai, T. Hara, S. Miura and H. Hosoda, *Intermetallics*, 2010, **18**, (12), 2275

21 S. R. Bharadwaj, S. N. Tripathi and M. S. Chandrasekharaiah, *J. Phase Equilib.*, 1995, **16**, (5), 460

22 J. R. Chelikowsky and K. E. Anderson, *J. Phys. Chem. Solids*, 1987, **48**, (2), 197

23 Y. Yamabe-Mitarai, T. Hara and H. Hosoda, *Mater. Sci. Forum*, 2003, **426–432**, 2267

24 Y. Yamabe-Mitarai, T. Hara, S. Miura and H. Hosoda, *Mater. Sci. Forum*, 2005, **475–479**, 1987

25 Y. Yamabe-Mitarai, T. Hara, S. Miura and H. Hosoda, *Metall. Mater. Trans. A*, 2012, **43**, (8), 2901

26 A. G. Paradkar, S. V. Kamat, A. K. Gogia and B. P. Kashyap, *Mater. Sci. Eng.: A*, 2007, **456**, (1–2), 292

27 A. Wadood, M. Takahashi, S. Takahashi, H. Hosoda and Y. Yamabe-Mitarai, *Mater. Sci. Eng.: A*, 2013, **564**, 34

28 A. Wadood, M. Takahashi, S. Takahashi, H. Hosoda and Y. Yamabe-Mitarai, 'Improvement of Mechanical and Shape Memory Properties of Ti-50Pt High Temperature Shape Memory Alloys by Addition of Group IV Elements', in "TMS2013 Supplemental Proceedings", San Antonio, John Wiley & Sons, Inc, Hoboken, New Jersey, USA, 2013, pp. 949–958

29 A. Wadood, M. Takahashi, S. Takahashi, H. Hosoda and Y. Yamabe-Mitarai, 'TiPt Based Shape Memory Alloys for High Temperature Material Applications', The 10th International Bhurban Conference on Applied Sciences & Technology (IBCAST), Islamabad, Pakistan, 15th–19th January, 2013

30 J. C. Slater, *J. Chem. Phys.*, 1964, **41**, (10), 3199

The Authors

Abdul Wadood is a postdoc researcher with the High Temperature Materials Unit, NIMS, Japan. He holds a PhD degree from the Tokyo Institute of Technology, Japan. He was awarded Tokyo Institute of Technology Tejima award for his scientific contribution in February 2014. In April 2014, he will join as assistant professor, Department of Materials Science and Engineering, Institute of Space Technology (IST), Pakistan. He completed his Master of Science at Ghulam Ishaq Khan Institute of Engineering Sciences and Technology (GIKI), Pakistan, and Bachelor of Engineering at University of Engineering and Technology (UET) Lahore, Pakistan. He worked for six years as a materials engineer at GIKI Institute, Pakistan. His research interests are the use of pgms in titanium based high-temperature shape memory alloys, oxidation and corrosion of metallic materials and the development of biomedical shape memory alloys.

Yoko Yamabe-Mitarai gained her PhD at the Tokyo Institute of Technology in 1994. After working on a JSPS fellowship in 1994 and 1995, she joined NIMS and engaged in research on the mechanical and functional properties of pgms, which are used in automotive engine spark plugs, aiming to grow single crystals for electronic devices in furnaces at ultra-high temperatures between 1400ºC and 2000ºC. Recent interests include high-temperature shape memory alloys using pgms which can operate at around 1000ºC.